A rotifer-derived paralytic compound prevents transmission of schistosomiasis to a mammalian host

Jiarong Gao[a,b,1], Ning Yang[c,1], Fred A. Lewis[d,2], Peter Yau[e], James J. Collins III[b,3], Jonathan V. Sweedler[c,4], Phillip A. Newmark[b,f,g,h,4]

[a]Cellular and Molecular Biology Program, University of Wisconsin-Madison, Madison, WI, USA. [b]Department of Cell and Developmental Biology, University of Illinois at Urbana-Champaign, Urbana, IL, USA. [c]Department of Chemistry, University of Illinois at Urbana-Champaign, Urbana, IL, USA. [d]Biomedical Research Institute, Rockville, MD, USA. [e]Roy J. Carver Biotechnology Center, University of Illinois at Urbana-Champaign, Urbana, IL, USA. [f]Howard Hughes Medical Institute, USA. [g]Morgridge Institute for Research, Madison, WI, USA. [h]Department of Integrative Biology, University of Wisconsin-Madison, Madison, WI, USA.

[1]These authors contributed equally

[2]Present address: Bernville, PA, USA

[3]Present Address: Department of Pharmacology, UT Southwestern Medical Center, Dallas, TX, USA

[4]To whom correspondence should be addressed: e-mail: jsweedle@illinois.edu; pnewmark@morgridge.org

Keywords: *Schistosoma mansoni* | *Rotaria rotatoria* | schistosomiasis

Abstract

Schistosomes are parasitic flatworms that infect over 200 million people, causing the neglected tropical disease, schistosomiasis. A single drug, praziquantel, is used to treat schistosome infection. Limitations in mass drug administration programs and the emergence of schistosomiasis in non-tropical areas indicate the need for new strategies to prevent infection. It has been known for several decades that rotifers colonizing the schistosome's snail intermediate host produce a water-soluble factor that paralyzes cercariae, the life-cycle stage infecting humans. In spite of its potential for preventing infection, the nature of this factor has remained obscure. Here, we report the purification and chemical characterization of Schistosome Paralysis Factor (SPF), a novel tetracyclic alkaloid produced by the rotifer *Rotaria rotatoria*. We show that this compound paralyzes schistosome cercariae and prevents infection, and does so more effectively than analogous compounds. This molecule provides new directions for understanding cercariae motility and new strategies for preventing schistosome infection.

32 **Introduction**

33 Schistosomiasis – caused by parasitic flatworms of the genus *Schistosoma* – is a major neglected
34 tropical disease, affecting over 200 million people, with over 700 million people at risk of
35 infection (1-3). Praziquantel is currently the only drug used for treating schistosomiasis.
36 Concerns about the emergence of drug resistance (4, 5) as well as limitations observed in mass
37 drug administration programs (6-9) highlight the need to devise new strategies for preventing
38 infection by these parasites. This need is amplified by the recent identification of people infected
39 with human/livestock hybrid schistosomes and the geographical expansion of schistosomiasis to
40 temperate regions (10-12).

41 Schistosomes have a complex life cycle that alternates between an intermediate host (snail) and a
42 definitive host (mammal) via two free-living, water-borne forms called miracidia and cercariae,
43 respectively (13) (Fig. 1A). For decades, inconsistency in cercarial production by snails and
44 infectivity of mammalian hosts has been observed in most schistosome laboratories (14).
45 Intriguingly, Stirewalt and Lewis reported that rotifer colonization on shells of the snail
46 intermediate host (*Biomphalaria glabrata*) significantly reduced cercariae output, motility, and
47 infectivity (15). Furthermore, they observed that cercarial motility was affected not only by the
48 presence of rotifers, but also by rotifer-conditioned water, indicating that rotifers released water-
49 soluble molecules with paralytic activity. Almost 40 years have passed since this important
50 finding, yet this factor's identity has remained a mystery.

Results and Discussion

Purification of the rotifer-derived compound. Encouraged by this anti-cercarial effect and its potential to prevent schistosome infection, we sought to purify this paralyzing agent. We isolated individual rotifers from snail shells and found two species, *Rotaria rotatoria* (Fig. 1B) and *Philodina acuticornis* (Fig. 1C), as previously reported (15). To identify which rotifer was responsible for the paralytic effect, we grew clonal isolates of each species, producing rotifer-conditioned artificial pond water (APW). Adding *Rotaria*-conditioned APW to freshly collected cercariae resulted in gradual paralysis within five minutes (Fig. 1D). Most cercariae stopped swimming and sank to the bottom of the dish. Tapping the dish could stimulate their movement, but their response was limited to writhing on the dish bottom or short-distance swimming before becoming paralyzed again. In contrast, *P. acuticornis*-conditioned water had no effect (Fig. 1E).

To purify the paralyzing agent, we performed molecular weight cut-off filtration (MWCO) of rotifer-conditioned water and found that the activity was present in the <650 Da fraction. The <650 Da filtrate was fractionated by reversed-phase high-performance liquid chromatography (RP-HPLC) (Fig. 2A) and each fraction was tested qualitatively (i.e., plus/minus) for paralytic activity on cercariae. Paralysis was only observed following treatment with a peak eluting at 25-27 min (Fig. 2B). As expected, this peak was detected only in *R. rotatoria*- but not *P. acuticornis*-conditioned water (Fig. 2B). Performing a second round of HPLC on this active fraction and assaying all the resulting peaks revealed a single peak (eluting at 24-26 min) with paralytic activity (Fig. 2C). A predominant signal of m/z 273.16 (M+H) in this peak was revealed by matrix-assisted laser desorption/ionization mass spectrometry (MALDI-MS) (Fig. 2D). Consistent with the paralysis assay, this signal (m/z 273.16) was detected exclusively in the fraction eluting at 24-26 min but not in the fractions before or after (Fig. 2E). These results

74 suggested that the component with m/z 273.16 was the paralyzing agent, which we named
75 "Schistosome Paralysis Factor" (SPF). We then determined the monoisotopic mass for
76 protonated SPF using high-resolution quadrupole time-of-flight (Q-TOF) MS, m/z 273.1595 (Fig.
77 2F), suggesting $C_{16}H_{20}N_2O_2$ as the best-fitting formula for SPF.

78 **SPF is a novel tetracyclic alkaloid.** To elucidate its structure, we purified ~0.1 mg SPF from 25
79 L *R. rotatoria*-conditioned water. Nuclear magnetic resonance (NMR) spectroscopy revealed a
80 novel tetracyclic structure. Briefly, ^{1}H spectra showed the presence of 19 protons in the
81 compound (Fig. S1), which agrees with the best-fitting formula and Hydrogen/Deuterium
82 exchange mass spectrometry (MS) analysis (Fig. S2). Heteronuclear single quantum coherence
83 spectroscopy **(**HSQC) revealed three methyl, two methylene, six methine groups, and five
84 quaternary carbons (Fig. S3). Total correlation spectrometry (TOCSY) showed that aliphatic
85 protons, except two methyl groups, are from one spin system (Fig. S4). The connectivity of the
86 neighboring groups was derived from correlation spectroscopy (COSY) and heteronuclear
87 multiple bond correlation (HMBC) spectra (Fig. S5 and S6). Overall, the aliphatic region is
88 composed of a dimethylpyrrolidine structure which is linked to an indole via a CH_2 group and an
89 oxygen. Nuclear Overhauser effect spectroscopy (NOESY) suggested (*R, S, S*) or (*S, R, R*)
90 configurations on the chiral centers (Fig. S7). Altogether, combined NMR analysis led to two
91 possible structures (Fig. 2G and H; Table S1).

92 **SPF and its analogs paralyze cercariae in a dose-dependent manner.** To test its dose
93 dependency, we examined the paralytic effect of serially diluted SPF on cercariae by quantifying
94 their movement over time. In the absence of SPF, over 82% of cercariae were free-swimming
95 over three minutes (Fig. 3A). In 2.5 nM SPF, the percentage of free-swimming cercariae dropped
96 to 67% at three-minutes post drug treatment. As the concentration of SPF increased, so did the

97 rate of paralysis, and more cercariae were paralyzed at the end of treatment. We observed
98 maximum effects in 250 nM and 2.5 μM SPF, with the majority of cercariae paralyzed within 30
99 s.

100 Two natural compounds isolated from *Streptomyces sp.*, ht-13-A and ht-13-B (16), are
101 structurally related to SPF. All three alkaloids share a novel oxepineindole framework fused with
102 a pyrrolidine ring (Fig. 3A-C). Although synthesis of SPF has not been achieved, total syntheses
103 of ht-13-A and ht-13-B have been reported (17-19). To test whether this shared tetracyclic
104 scaffold is responsible for the paralytic effect, we analyzed structure-activity relationships by
105 using ht-13-A, ht-13-B, three ht-13-A derivatives (18), and one epimer in cercarial paralysis
106 assays. Importantly, ht-13-A, although not as potent as SPF, also had a paralytic effect on
107 cercariae (Fig. 3B). In contrast, ht-13-B did not paralyze cercariae, suggesting that the extra
108 methyl group disrupts interaction with the target (Fig. 3C). Of the three ht-13-A analogs, only ht-
109 13-A-pr effectively paralyzed cercariae; it was more potent than ht-13-A, indicating that the
110 nature of the side chain is important for proper target interaction (Fig. 3D-E). In contrast to ht-
111 13-A, the epimer was unable to paralyze cercariae, supporting the (*R, S*) configuration of SPF at
112 C12, 13 (Fig. 2G).

113 **SPF prevents mammalian infection.** Since motility of the cercarial tail is essential for
114 swimming and provides force for skin penetration (20-22), we examined whether SPF prevented
115 infection. We treated ~200 cercariae with different concentrations of SPF for 10 mins, and tested
116 their ability to infect mice after a 30-min exposure to their tails (N=6 for each condition). Six-
117 weeks post infection, we euthanized the mice, counted schistosomes recovered after hepatic
118 portal vein perfusion, and examined liver pathology. From controls, we recovered 83 adult
119 worms on average (Fig. 4A), consistent with typical recoveries of ~40% (23). Livers from these

120 mice appeared dark and contained extensive granulomas (Fig. 4A). In contrast, we did not
121 recover any adult worms from mice after treatment with 250 nM or 2.5 μM SPF (Fig. 4B) and no
122 granulomas were observed (Fig. 4A). Histological examination confirmed that these livers were
123 free of schistosome eggs (Fig. 4E), suggesting complete inhibition of infection. These data are
124 consistent with the full paralysis observed after treatment with 250 nM or 2.5 μM SPF (Fig. 3A).
125 Although 25 nM SPF paralyzed most cercariae *in vitro*, the effects on mouse infection were not
126 as severe (Fig. 4A). Mechanical and/or chemical stimuli from mouse tails may overcome SPF-
127 induced paralytic effects at low SPF concentrations. Notably, neither Ht-13-A nor Ht-13-A-pr
128 blocked infection as completely as 250 nM SPF, even at 25 μM (Fig. 4A, C, D, F, G). Under
129 more realistic infection conditions, in which mouse tails were lifted 1-2 cm from the bottom of
130 the test tube containing cercariae, so they had to swim actively towards the tail to infect the
131 mouse, Ht-13-A and Ht-13-A-pr were still not as effective as SPF, which completely blocked
132 infection (Fig. S8).

133 **Conclusion**

134 This work has identified a novel tetracyclic alkaloid, produced by the rotifer *R. rotatoria,* that
135 paralyzes the infective larvae of schistosomes. Although its mechanism of action remains
136 unknown, its chemical structure provides important clues. SPF contains a serotonin backbone,
137 suggesting that SPF might antagonize serotonin signaling, perhaps via G protein-coupled
138 receptors (GPCRs) or serotonin-gated channels. Consistent with this idea, the structurally related
139 compounds, ht-13-A and ht-13-B, bind several human serotonin receptors (16). In schistosomes,
140 serotonin has been implicated in neuromuscular functions in multiple life stages (24-27);
141 knocking down a serotonergic GPCR (Sm5HTR) in schistosomulae and adult worms led to

142 decreased movement (28). Interestingly, praziquantel partially activates the human serotonin
143 receptor, HT2BR, suggesting that it may also target schistosome serotonergic GPCRs (29).

144 The chemical ecology underlying *R. rotatoria*'s production of SPF is also unclear. Whether SPF
145 is used naturally to combat other aquatic creatures (e.g., to prevent other rotifers from colonizing
146 areas where *R. rotaria* live) and, thus, the effect on schistosome cercariae is indirect, or whether
147 SPF benefits the rotifer's commensal host will require further study. Given that the previously
148 described related compounds are produced by *Streptomyces sp*.(16), it will also be important to
149 examine the possibility that SPF is not directly produced the rotifer, but rather by constituent(s)
150 of its own microbiome. In the past few decades, the discovery and development of natural
151 products have helped combat parasitic diseases (30). Based on its ability to block infection, SPF
152 holds great promise as an anti-schistosomal agent. Identifying the biologically active chemical
153 scaffolds and understanding SPF's mode of action are expected to provide important clues for
154 preventing schistosomiasis.

155 **Materials and Methods**

156 **Artificial pond water.** Four stock solutions were prepared to make artificial pond water (31): 1)
157 0.25 g/L $FeCl_3 \cdot 6H_2O$, 2) 12.9 g/L $CaCl_2 \cdot 2H_2O$, 3) 10g/L $MgSO_4 \cdot 7H_2O$, and 4) 34 g/L
158 KH_2PO_4 1.5 g/L $(NH_4)_2SO_4$, pH 7.2. For 1L artificial pond water, we added 0.5 mL of $FeCl_3$
159 solution, 2.5 mL $CaCl_2$ solution, 2.5 mL $MgSO_4$ solution and 1.25 mL phosphate buffer.

160 **Obtaining *S. mansoni* cercariae.** Infected *B. glabrata* snails provided by Biomedical Research
161 Institute (BRI, Rockville, MD) were maintained in artificial pond water and fed Layer Crumbles
162 (chicken feed) (Rural King, Mattoon, IL). To obtain *S. mansoni* cercariae, *B. glabrata* snails
163 were exposed to light at 26°C for 1-2 hrs. Artificial pond water containing cercariae was passed
164 through 100 μm cell strainer (Falcon) to remove snail food and feces. Cercariae were then
165 collected using custom-made 20 μm cell strainers.

166 **Rotifer culture.** Since both rotifer species reproduce parthenogenetically, we clonally expanded
167 each species into one-liter cultures from a single rotifer. Individual rotifers (*R. rotatoria* and *P.*
168 *acuticornis*) were initially isolated from the shell of *B. glabrata* and cultured in artificial pond
169 water in 24-well plates. Each individual colony was expanded into ever-larger culture volumes
170 and ultimately maintained in two-liter flasks. Both species were fed Roti-rich liquid invertebrate
171 food (Florida Aqua Farms Inc). Rotifer-conditioned water was collected every month by filtering
172 out the rotifers using a 20 μm cell strainer. Conditioned water from *R. rotatoria* paralyzed
173 cercariae completely within 3-5 minutes, resembling treatment with 25 nM purified SPF, and
174 suggesting an SPF concentration in the range of tens of nM. Filtered rotifers were then passaged
175 to fresh artificial pond water to propagate the cultures.

176 **Crude rotifer-conditioned water preparation.** One liter rotifer media was lyophilized,
177 reconstituted with 50 mL dH_2O and filtered through 10,000 and 650 (MWCO) Pall Minimate
178 TFF Capsules with Omega membrane (Ann Arbor, MI). Filtrate (<650 Da) was freeze dried. For
179 RP-HPLC, 300 mg of the dried material was dissolved in dH_2O and run on a RP-HPLC – Merck
180 Chromolith semi-prep RP-18e column (Darmstadt, Germany) at 5 ml/min using a gradient of
181 100% A to 60% B in 60 min. 10 mL fractions were collected and assayed for biological activity.
182 Fractions containing biological activity were saved for further study.

183 **Further purification of rotifer media.** The bioactive fractions were pooled, freeze dried with
184 SpeedVac (Savant, MA), reconstituted with 500 μL dH_2O and injected into a 4.6mm diameter ×
185 25cm Symmetry column (Waters, MA). Breeze2 analytical LC system (Waters, MA) was
186 employed for separation at 0.5 ml/min with the following solvents and gradients: Solvent A,
187 0.1% formic acid (FA); solvent B, methanol with 0.1% FA; 0—10 min 0—10% B, 10—30 min
188 10—35% B, 30—33 min 35—80% B, 33—37 min 80—80% B, 37—40 min 80—0% B. Eluents
189 were collected manually based on peak elution. All fractions were lyophilized, reconstituted with
190 water and analyzed with MALDI-MS. Fractions containing biological activity were saved for
191 future use.

192 **Matrix-assisted laser desorption/ionization mass spectrometry (MALDI-MS) analysis.** For
193 each collected fraction, 1 μL of sample solution was spotted on ground steel MALDI target and
194 mixed with 1 μL of alpha-cyano-4-hydroxy-cinnamic acid (CHCA, Sigma-Aldrich, MO)
195 solution (10 mg/mL CHCA in 50% acetonitrile solution with 0.005% trifluoroacetic acid). Mass
196 calibration, spectra acquisition and analysis were performed under conditions as previously
197 described (32).

198 **High-resolution quadrupole time-of-flight mass spectrometry (Q-TOF MS) analysis.** 1 μL
199 of the bioactive fraction was separated on a Magic 0.1 × 150mm column (Michrom, CA) and
200 analyzed with maXis 4G mass spectrometer (Bruker, MA) using previously established methods
201 for metabolite study (33). The separation was performed at 300 nl/min by use of solvent A (95%
202 water, 5% acetonitrile with 0.1% FA) and solvent B (5% water, 95% acetonitrile with 0.1% FA)
203 with the following gradient conditions: 0—5 min 4% B, 5—50 min 4—50% B, 50—52 min
204 50—90% B, 52—60 min 90% B, 60—70 min 90—4% B, 70—90 min 4% B.

205 **Hydrogen/deuterium (H/D) exchange analysis.** Acidified deuterated methanol (CD_3OD,
206 methanol—d4, Sigma—Aldrich, MO) was made by adding 1 μL of deuterated FA into 1 mL of
207 CD_3OD. 2 μL of the bioactive fractions were added into 18 μL of acidified methanol above. 15
208 μL of the mixture were analyzed by direct infusion into a modified 11 Tesla FTMS (Thermo
209 Scientific, MA) through NanoMate robot (Advion, NY) (34). Full spectra were acquired with
210 resolution set at 100k.

211 **Nuclear magnetic resonance (NMR) analysis.** Purified bioactive materials were dissolved in
212 250 μL of CD_3OD and transferred into a 5 mm Shigemi NMR tube with a glass magnetic plug
213 with susceptibility matched to CD_3OD on the bottom. All NMR data were collected at 40°C on

214 an Agilent VNMRS 750 MHz spectrometer equipped with a 5 mm Varian indirect detection
215 probe with z gradient capability. Collected NMR data included 1H spectrum, gradient selected
216 correlation spectroscopy (gCOSY), total correlation spectroscopy (TOCSY), nuclear Overhauser
217 enhancement spectroscopy (NOESY) with a mixing time of 500 ms, heteronuclear single
218 quantum coherence spectroscopy (^{1}H—^{13}C HSQC) and heteronuclear multiple-bond correlation
219 spectroscopy (^{1}H—^{13}C HMBC). The NMR spectra were analyzed using Mnova NMR software
220 (Mestrelab Research, Spain).

221 **Determination of SPF concentration.** The proton quantification experiments were performed at
222 23°C on an Agilent 750 MHz VNMRS NMR spectrometer equipped with a 5 mm triple-
223 resonance (^{1}H/^{13}C/^{15}N) indirect-detection probe with XYZ PFG gradient capability. The probe
224 was calibrated using the qEstimate tool in the Agilent VnmrJ4.2 software with a known standard.
225 The proton spectrum of the sample was collected with a 90-degree pulse angle of 8.5 ms, 16
226 scans and 10.4 s delay between scans. The Agilent VnmrJ4.2 software was used to determine the
227 concentration of the sample based on the integration values of proton peaks. A total of 5 well-
228 resolved proton peaks (7.12ppm (1H), ~6.89ppm (2H), 4.41 (1H), 3.83 (3H), and ~3.58 (2H))
229 was used, and the concentration of the sample was 1.55 ± 0.07 mM. All concentrations used in
230 the cercarial paralysis assay were calculated based on this value.

231 **Cercarial paralysis assay.** To capture the whole field while avoiding excess reflected light in a
232 well, we used the lid of 96-well plate (Costar). 40 μL of artificial pond water containing ~50
233 cercariae were added to each shallow well on the lid. 10 μL of SPF (dissolved in APW) was then
234 added to reach the final concentration indicated. Using a high-speed camera (Olympus i-SPEED
235 TR), attached to a stereomicroscope (Leica MZ125), we recorded cercariae movement at 20-60

236 fps at 1.25X magnification just prior to addition of test compounds until 3-4 min after treatment
237 started. Raw movies were converted to .avi files using i-SPEED Viewer and compressed into
238 JPEG format using ImageJ (addition of compound is considered time 0). We then counted the
239 numbers of free swimming/paralyzed cercariae every 5 s for 1 min and every 30 s thereafter for 3
240 min. The number of dead cercariae (those that never swim before and after SPF treatment) were
241 subtracted from data. Experiments were performed in biological triplicate.

242 **Mouse infectivity assay.** Mouse infections were performed by exposing mouse tails to *S.*
243 *mansoni* cercariae according to standard protocol from BRI(23) with slight modifications.
244 Briefly, we secured mice in rodent restrainers (Thomas Scientific, Cat #551-BSRR) and put them
245 vertically on top of a rack with grids. We pipetted 100 μL of each drug at proper concentration
246 into a skinny glass tube (Fisher Scientific, Cat #14-958A) inside a 12 X 75 mm holding glass
247 tube (VWR, Cat # 47729-570). 300 μL of APW containing ~200 cercariae were pipetted into
248 each skinny tube and incubated for 10 mins before we inserted the mouse tail. Mouse tails were
249 wiped with APW-moistened Kimwipes, inserted into the skinny tube, and exposed to cercariae
250 for 30 mins. The mouse tail was touching the bottom of the test tube unless otherwise specified.
251 We euthanized and perfused these mice six week-post infection according to standard
252 protocols(23). For each drug, we initially used three mice for controls (APW only) and three
253 mice for each concentration tested except for 25 nM Ht-13-A and Ht-13-A-pr. We then repeated
254 the experiments again with three mice for each condition. In addition to that, we included six
255 mice for 25 nM Ht-13-A and Ht-13-A-pr.

256 Adult worms were recovered by hepatic portal vein perfusion and briefly incubated in 2.5%
257 Tricaine (Sigma) to separate males and females. We counted total numbers of adult worms under

258 a stereomicroscope (Leica MZ75). Livers from infected mice were fixed in 4% formaldehyde in
259 PBS overnight. Largest liver lobes (left lobe) were submitted to University of Wisconsin-
260 Madison Histology Core Facility for sectioning and Hematoxylin and Eosin staining. Each left
261 lobe was evenly cut into 4-6 pieces and paraffin embedded on a large cassette. One slide (4-6
262 liver sections) for each liver was used for histological examination, which provided a
263 representative view throughout the whole liver lobe. We took a tiled image of the whole slide
264 using a Zeiss Axio Zoom microscope and used ImageJ to determine the area of each section.
265 Total numbers of eggs in each section were counted and normalized to the area.

266 In adherence to the Animal Welfare Act and the Public Health Service Policy on Humane Care
267 and Use of Laboratory Animals, all experiments with and care of mice were performed in
268 accordance with protocols approved by the Institutional Animal Care and Use Committee
269 (IACUC) of the University of Wisconsin-Madison (protocol approval number M005569).

270 **Statistical analysis.** GraphPad Prism (Version 7) was used for all statistical analyses. One-way
271 ANOVA test followed by Dunnett's multiple comparison test was used. Mean ± S.D. is shown in
272 all figures.

Acknowledgments. *B. glabrata* snails were provided by the NIAID Schistosomiasis Resource Center of the Biomedical Research Institute (Rockville, MD) through NIH-NIAID Contract HHSN272201700014I for distribution through BEI Resources. We thank: Melanie Issigonis, Umair Khan, Jayhun Lee, and Tania Rozario for helpful discussions and comments on the manuscript; Tracy Chong and Jayhun Lee for help maintaining the schistosome life cycle; Melanie Issigonis for solving the pond water crisis; Björn Söderberg and Yanxing Jia for providing Ht-13-A, -B, and derivatives; Lingyang Zhu for expert assistance with NMR; Brian Imai for assistance with SPF purification; as well as Peg Stirewalt, James Leef, Tom Nerad, and Paul Mazzocchi for their early efforts to help solve this puzzle.

References

1. WHO (2017) Schistosomiasis and soil-transmitted helminthiases: number of people treated in 2016. *Wkly Epidemiol Rec* 92(49):749-760.
2. Steinmann P, Keiser J, Bos R, Tanner M, & Utzinger J (2006) Schistosomiasis and water resources development: systematic review, meta-analysis, and estimates of people at risk. *The Lancet. Infectious diseases* 6(7):411-425.
3. Colley DG, Bustinduy AL, Secor WE, & King CH (2014) Human schistosomiasis. *Lancet* 383(9541):2253-2264.
4. Doenhoff MJ, Cioli D, & Utzinger J (2008) Praziquantel: mechanisms of action, resistance and new derivatives for schistosomiasis. *Current opinion in infectious diseases* 21(6):659-667.
5. Wang W, Wang L, & Liang YS (2012) Susceptibility or resistance of praziquantel in human schistosomiasis: a review. *Parasitol Res* 111(5):1871-1877.
6. Assare RK*, et al.* (2016) Sustaining Control of Schistosomiasis Mansoni in Western Cote d'Ivoire: Results from a SCORE Study, One Year after Initial Praziquantel Administration. *PLoS Negl Trop Dis* 10(1):e0004329.
7. Ross AG*, et al.* (2015) Can mass drug administration lead to the sustainable control of schistosomiasis? *J Infect Dis* 211(2):283-289.
8. Inobaya MT, Olveda RM, Chau TN, Olveda DU, & Ross AG (2014) Prevention and control of schistosomiasis: a current perspective. *Res Rep Trop Med* 2014(5):65-75.
9. Crellen T*, et al.* (2016) Reduced Efficacy of Praziquantel Against *Schistosoma mansoni* Is Associated With Multiple Rounds of Mass Drug Administration. *Clin Infect Dis* 63(9):1151-1159.
10. Kincaid-Smith J, Rey O, Toulza E, Berry A, & Boissier J (2017) Emerging Schistosomiasis in Europe: A Need to Quantify the Risks. *Trends in parasitology* 33(8):600-609.
11. Leger E & Webster JP (2017) Hybridizations within the Genus *Schistosoma*: implications for evolution, epidemiology and control. *Parasitology* 144(1):65-80.
12. Webster BL, Diaw OT, Seye MM, Webster JP, & Rollinson D (2013) Introgressive hybridization of *Schistosoma haematobium* group species in Senegal: species barrier break down between ruminant and human schistosomes. *PLoS Negl Trop Dis* 7(4):e2110.
13. Basch PF (1991) Schistosomes : development, reproduction, and host relations. *New York : Oxford University Press*:248 p.
14. Lewis FA, Stirewalt MA, Souza CP, & Gazzinelli G (1986) Large-scale laboratory maintenance of *Schistosoma mansoni*, with observations on three schistosome/snail host combinations. *J Parasitol* 72(6):813-829.
15. Stirewalt M & Lewis FA (1981) *Schistosoma mansoni*: effect of rotifers on cercarial output, motility and infectivity. *Int J Parasitol* 11(4):301-308.
16. Kamigauchi T & Yasui M (2000) WO/2000/059909.
17. Zhang YL, McArdle IW, Hubbard JW, Akhmedov NG, & Soderberg BCG (2016) Total synthesis of the tetracyclic indole alkaloid ht-13-A. *Tetrahedron Lett* 57(26):2865-2867.
18. Tao P, Chen Z, & Jia Y (2016) A concise gram-scale synthesis of ht-13-A via a rhodium-catalyzed intramolecular C-H activation reaction. *Chem Commun (Camb)* 52(75):11300-11303.

326 19. Zhang Y, Hubbard JW, Akhmedov NG, Petersen JL, & Soderberg BC (2015) Total
327 synthesis of the tetracyclic indole alkaloid ht-13-B. *J Org Chem* 80(9):4783-4790.
328 20. Haas W (1992) Physiological analysis of cercarial behavior. *J Parasitol* 78(2):243-255.
329 21. Haas W (2003) Parasitic worms: strategies of host finding, recognition and invasion.
330 *Zoology (Jena)* 106(4):349-364.
331 22. Whitfield PJ, Bartlett A, Khammo N, & Clothier RH (2003) Age-dependent survival and
332 infectivity of *Schistosoma mansoni* cercariae. *Parasitology* 127(Pt 1):29-35.
333 23. Lewis F (2001) Schistosomiasis. *Curr Protoc Immunol* Chapter 19:Unit 19 11.
334 24. Ribeiro P, Gupta V, & El-Sakkary N (2012) Biogenic amines and the control of
335 neuromuscular signaling in schistosomes. *Invertebrate neuroscience : IN* 12(1):13-28.
336 25. Boyle JP, Zaide JV, & Yoshino TP (2000) *Schistosoma mansoni*: effects of serotonin and
337 serotonin receptor antagonists on motility and length of primary sporocysts in vitro. *Exp*
338 *Parasitol* 94(4):217-226.
339 26. Boyle JP & Yoshino TP (2005) Serotonin-induced muscular activity in *Schistosoma*
340 *mansoni* larval stages: importance of 5-HT transport and role in daughter sporocyst
341 production. *J Parasitol* 91(3):542-550.
342 27. Chan JD*, et al.* (2016) A Miniaturized Screen of a *Schistosoma mansoni* Serotonergic G
343 Protein-Coupled Receptor Identifies Novel Classes of Parasite-Selective Inhibitors. *PLoS*
344 *Pathog* 12(5):e1005651.
345 28. Patocka N, Sharma N, Rashid M, & Ribeiro P (2014) Serotonin signaling in *Schistosoma*
346 *mansoni*: a serotonin-activated G protein-coupled receptor controls parasite movement.
347 *PLoS Pathog* 10(1):e1003878.
348 29. Chan JD*, et al.* (2017) The anthelmintic praziquantel is a human serotoninergic G-
349 protein-coupled receptor ligand. *Nat Commun* 8(1):1910.
350 30. Shen B (2015) A New Golden Age of Natural Products Drug Discovery. *Cell*
351 163(6):1297-1300.
352 31. Collins JJ, 3rd, King RS, Cogswell A, Williams DL, & Newmark PA (2011) An atlas for
353 *Schistosoma mansoni* organs and life-cycle stages using cell type-specific markers and
354 confocal microscopy. *PLoS Negl Trop Dis* 5(3):e1009.
355 32. Tillmaand EG*, et al.* (2015) Peptidomics and Secretomics of the Mammalian Peripheral
356 Sensory-Motor System. *J Am Soc Mass Spectrom* 26(12):2051-2061.
357 33. Aerts JT*, et al.* (2014) Patch clamp electrophysiology and capillary electrophoresis-mass
358 spectrometry metabolomics for single cell characterization. *Anal Chem* 86(6):3203-3208.
359 34. Lee JE*, et al.* (2010) Endogenous peptide discovery of the rat circadian clock: a focused
360 study of the suprachiasmatic nucleus by ultrahigh performance tandem mass
361 spectrometry. *Mol Cell Proteomics* 9(2):285-297.
362 35. Collins JJ, 3rd & Newmark PA (2013) It's no fluke: the planarian as a model for
363 understanding schistosomes. *PLoS Pathog* 9(7):e1003396.

364

365 **Figures**

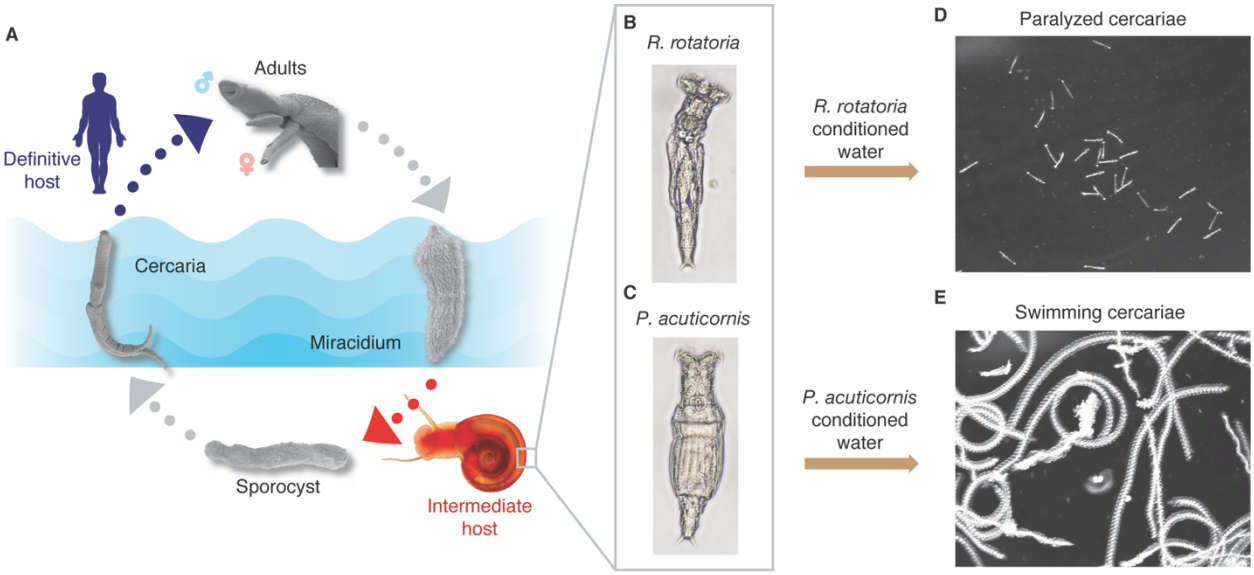

366

367 Fig. 1. *R. rotatoria*-conditioned water paralyzes *S. mansoni* cercariae. (*A*) Life cycle of *S.*
368 *mansoni*. Adult parasites, residing in the mammalian host vasculature, lay eggs (not shown).
369 Upon exposure to fresh water, eggs release miracidia, which infect the appropriate snail host.
370 Inside the snail the parasite reproduces asexually, ultimately producing large numbers of free-
371 swimming infective larvae (cercariae) that can penetrate mammalian skin to continue the life
372 cycle (adapted from (35)). (*B* and *C*), Bright-field microscopy images of *R. rotatoria* and *P.*
373 *acuticornis*. (*D* and *E*) Maximum intensity projection (5 s, 150 frames) of cercariae motility after
374 treatment with *R. rotatoria*- or *P. acuticornis*- conditioned water.

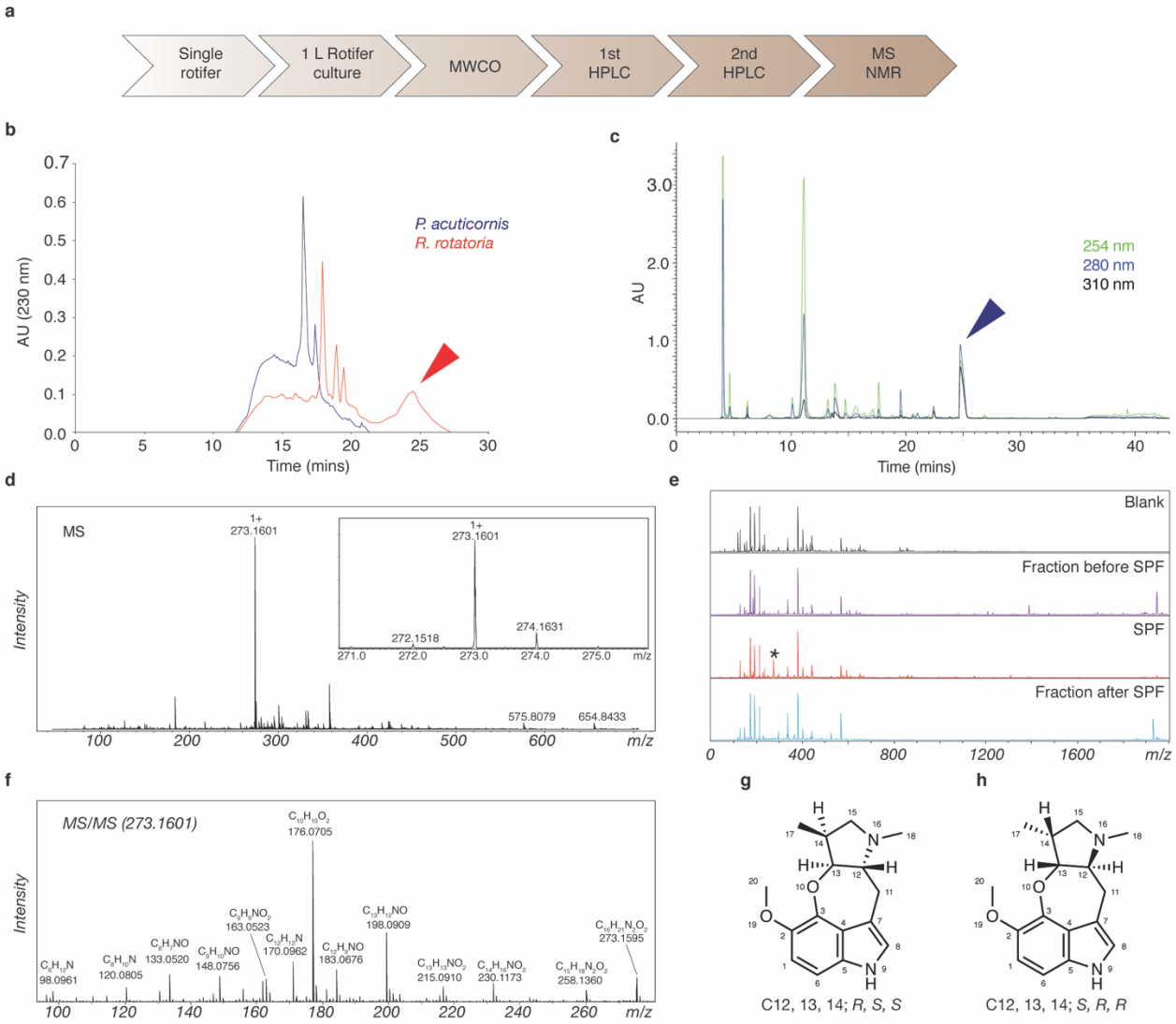

Fig. 2. SPF is a novel tetracyclic alkaloid. (*A*) Flowchart for SPF purification. (*B*) 1st HPLC plots of *R. rotatoria*- and *P. acuticornis*-conditioned water. All fractions were tested for bioactivity; the red arrowhead indicates the only active peak. (*C*) 2nd HPLC plot of the bioactive fraction (red arrowhead in *B*). All peaks were tested for bio activity; the blue arrowhead indicates the only peak containing activity. (*D*) MS showing the dominant signal of m/z 273.1601 from the peak (blue arrowhead). (*E*) MS plots showing this signal (asterisk, m/z 273.1601) was only detected in the fraction eluting at 24-26 min. (*F*) Tandem MS acquired from high-resolution Q-TOF analysis. (*G* and *H*) NOESY resolved the relative stereochemistry of three chiral centers and narrowed it down to two possible configurations.

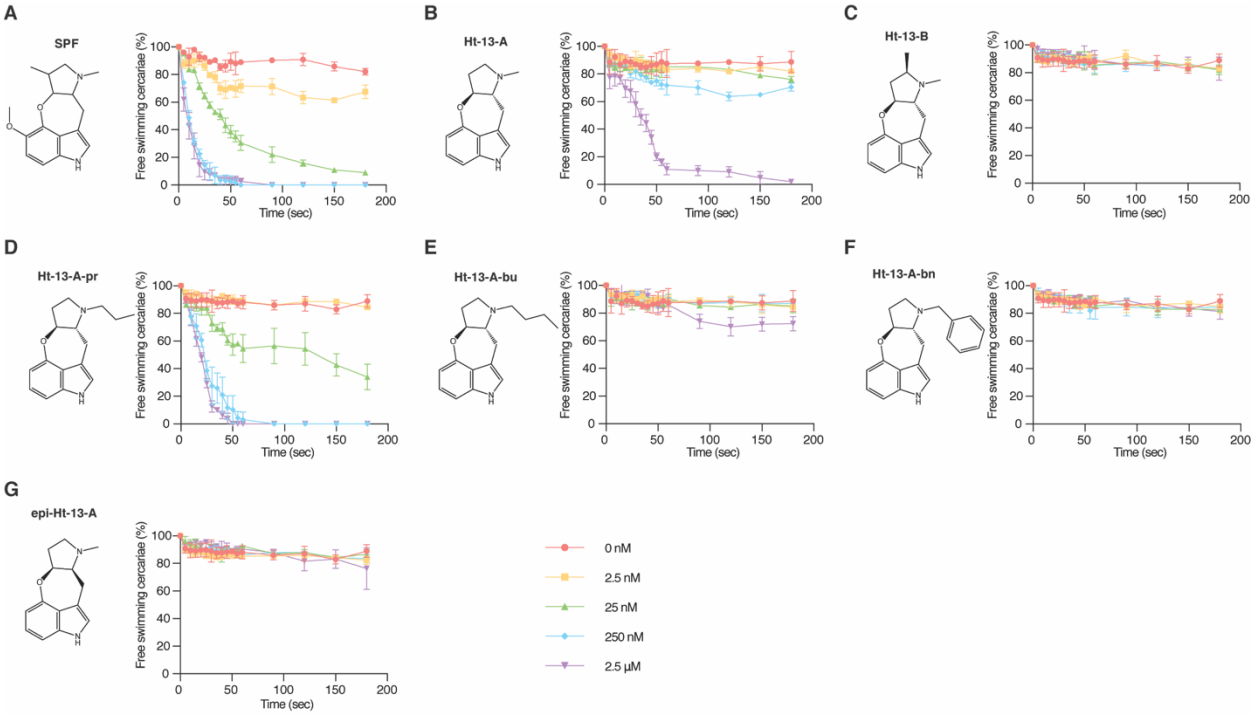

Fig. 3. Structure-activity relationships of SPF and related compounds as measured by cercarial motility assays. (*A*-*G*), Percentage of cercariae (~50) continuing to swim over three minutes after addition of each compound at specified final concentrations. Triplicates were performed. Data are mean ± S.D.

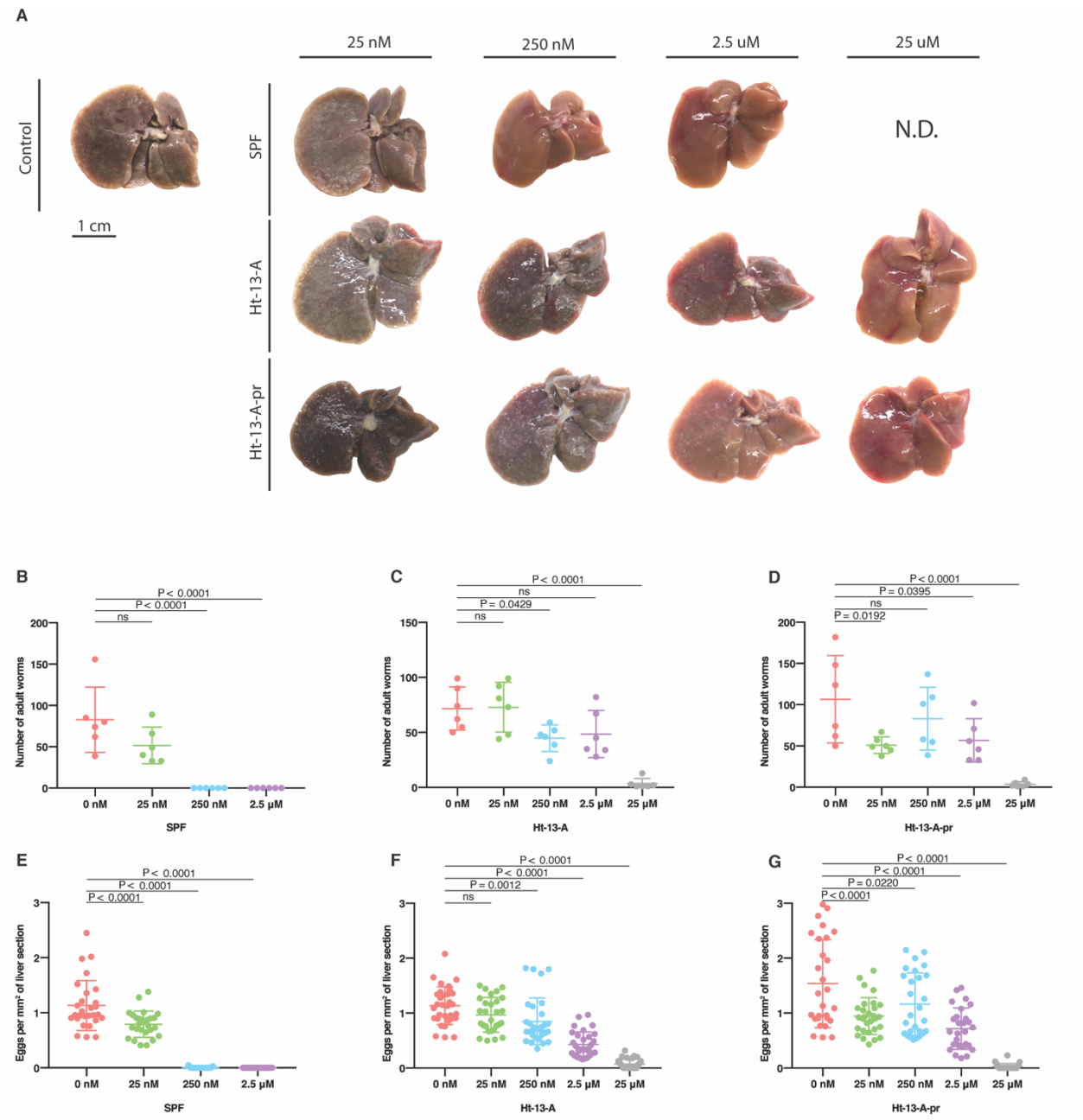

Fig. 4. Treating cercariae with SPF, Ht-13-A or Ht-13-A-pr blocks schistosome infection and alleviates pathology. (*A*) Representative livers (post perfusion) from mice (N=6) exposed to drug-treated cercariae. Livers from mice treated with control and lower drug concentrations were darker in color and contained more granulomas (white spots). With higher drug concentrations, livers had normal morphologies with few or no granulomas. 25 μM SPF treatment was not determined (N.D.) due to limited amounts of purified SPF. (*B-D*) Numbers of adult worms recovered from exposed mice (two experiments for each drug, 6 mice total for each condition). (*E-G*) Numbers of schistosome eggs per area (/mm^2) from liver sections (4-6 sections per mouse). Data (*B-G*) are mean ± S.D. Statistics: One-way ANOVA, post Dunnett's test.